AIP | Applied Physics Letters

Tunneling magnetoresistance in Fe3Si/MgO/Fe3Si(001) magnetic tunnel junctions

L. L. Tao, S. H. Liang, D. P. Liu, H. X. Wei, Jian Wang, and X. F. Han

Citation: Applied Physics Letters **104**, 172406 (2014); doi: 10.1063/1.4874837
View online: http://dx.doi.org/10.1063/1.4874837
View Table of Contents: http://scitation.aip.org/content/aip/journal/apl/104/17?ver=pdfcov
Published by the AIP Publishing

APPLIED PHYSICS LETTERS **104**, 172406 (2014)

Tunneling magnetoresistance in $Fe_3Si/MgO/Fe_3Si(001)$ magnetic tunnel junctions

L. L. Tao,[1] S. H. Liang,[1] D. P. Liu,[1] H. X. Wei,[1] Jian Wang,[2] and X. F. Han[1,a)]
[1]*Beijing National Laboratory for Condensed Matter Physics, Institute of Physics, Chinese Academy of Sciences, Beijing 100190, China*
[2]*Department of Physics and the Center of Theoretical and Computational Physics, The University of Hong Kong, Hong Kong, China*

(Received 27 March 2014; accepted 21 April 2014; published online 1 May 2014)

We present a theoretical study of the tunneling magnetoresistance (TMR) and spin-polarized transport in $Fe_3Si/MgO/Fe_3Si(001)$ magnetic tunnel junction (MTJ). It is found that the spin-polarized conductance and bias-dependent TMR ratios are rather sensitive to the structure of Fe_3Si electrode. From the symmetry analysis of the band structures, we found that there is no spin-polarized Δ_1 symmetry bands crossing the Fermi level for the cubic Fe_3Si. In contrast, the tetragonal Fe_3Si driven by in-plane strain reveals half-metal nature in terms of Δ_1 state. The giant TMR ratios are predicted for both MTJs with cubic and tetragonal Fe_3Si electrodes under zero bias. However, the giant TMR ratio resulting from interface resonant transmission for the former decreases rapidly with the bias. For the latter, the giant TMR ratio can maintain up to larger bias due to coherent transmission through the majority-spin Δ_1 channel. © *2014 AIP Publishing LLC*.
[http://dx.doi.org/10.1063/1.4874837]

The phenomenon of tunnel magnetoresistance (TMR) observed in magnetic tunnel junctions (MTJs) has been extensively investigated for decades, due to its rich physics and potential application in spintronic devices.[1] MTJ devices have several designs including the in-plane MTJ and perpendicular MTJ (p-MTJ), depending on the ferromagnetic electrodes possessing an in-plane or perpendicular magnetic easy axis. The room-temperature TMR ratio in excess of 600% has been achieved in the MgO-based in-plane MTJ[2] after the prediction of first-principles calculation.[3,4] The p-MTJ can be used for current-induced magnetization switching using spin-transfer torque (STT) effect[5,6] and has several advantages such as higher thermal stability and lower switching current density as compared with in-plane MTJ,[7] which are favorable in the applications for STT-based magnetic random access memory (STT-MRAM).[8,9] The critical switching current density J_c and thermal stability are the two key parameters characterizing the performance of the p-MTJ while maintaining the high TMR ratio. J_c is proportional to the Gilbert damping constant α and saturation magnetization M_s as $J_c \propto \alpha M_s$.[7] In this regard, $D0_3$-type Fe_3Si with uniaxial magnetic anisotropy is a promising candidate as a ferromagnetic electrode of p-MTJ due to its lower M_s and smaller α than that of NiFe (Py) or CoFe alloy,[10] and thus possibly achieving lower J_c. In addition, the high Curie temperature of $\sim$800 K as well as high spin polarization of $\sim$45%[11] makes Fe_3Si a better material as ferromagnetic electrodes of spintronic devices. Very recently, Fe_3Si has been explored as ferromagnetic electrode for the MTJ using amorphous Al-O barrier[12] and the room-temperature TMR ratio of $\sim$20% has been observed. Moreover, Fe_3Si was found to have an out-of-plane magnetization easy axis on MgO(001) substrate,[13] which favors the thermal stability of p-MTJ required for data non-volatility.

Besides switching current density and thermal stability, another important device merit of a MTJ is the TMR ratio. A natural question to ask is whether the MTJs with Fe_3Si electrode can yield giant TMR ratio. To answer this question, we have carried out a theoretical study on the quantum transport in a $Fe_3Si/MgO/Fe_3Si$ MTJ with two structures of Fe_3Si electrode. Our results show that for the MTJ with cubic Fe_3Si electrode, the zero-bias TMR ratio reaches 5000%. However, the giant TMR ratio decreases rapidly as the bias is turned on. In contrast, for the MTJ with tetragonal Fe_3Si electrode driven by in-plane strain, the zero-bias TMR ratio can reach 2000%. Importantly, this giant TMR ratio can sustain much larger bias. Analysis of symmetry-resolved band structures, electronic structures and transport in momentum space provide clear understanding of these results.

Our quantum transport calculation is based on Nonequilibrium Green's Function-density functional theory (NEGF-DFT) method that combines real-space DFT with the Keldysh NEGF formalism, as implemented in Nanodcal package. For more technical details, we refer interested readers to the original literature.[14] The spin-polarized conductance G_σ is given by Landauer-Büttiker formula

$$G_\sigma = \frac{e^2}{h}\sum_{\mathbf{k}_\parallel} T_\sigma(\mathbf{k}_\parallel, E_F), \tag{1}$$

where $T_\sigma(\mathbf{k}_\parallel, E_F)$ is the transmission coefficient at the Fermi level E_F with spin σ ($\sigma = \uparrow, \downarrow$) and transverse Bloch wave vector $\mathbf{k}_\parallel = (k_x, k_y)$ due to the transverse periodicity, e the electron charge, and h the Planck's constant. We used a $10 \times 10\, \mathbf{k}_\parallel$ mesh to converge the density matrix and a $400 \times 400\, \mathbf{k}_\parallel$ mesh for evaluating transmission coefficients of all spin channels. The valence electrons are treated by

a)Electronic mail: xfhan@iphy.ac.cn

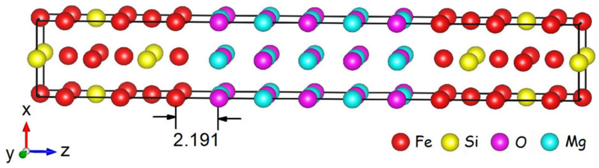

FIG. 1. Optimized atomic structure of a $Fe_3Si/MgO/Fe_3Si$ MTJ model. The transport direction is along the *z*-axis while the MTJ is periodic along the *x*- and *y*-directions. The optimized Fe-O distance (in unit of Å) is marked.

linear combination of atomic orbital basis with double-ζ plus polarization basis for all the atoms. The local density approximation as parameterized by Perdew and Zunger is used for the exchange-correlation potential.[15]

The MTJ device model investigated in this work is a two-probe tunnel junction, consisting of two semi-infinite Fe_3Si electrodes sandwiching several monolayers (ML) of MgO barriers as shown in Fig. 1. The atomic structures of central region are fully relaxed using the DFT based VASP electronic package.[16] The in-plane lattice constant of the junction is fixed at 3.997 Å, corresponding to $1/\sqrt{2}$ of experimental value (5.653 Å) of Fe_3Si. Thus, the lattice mismatch between $Fe_3Si(001)$ and MgO(001) (4.21 Å) rotated by 45° is about 5%. The optimized Fe-O distance is found to be 2.191 Å. Note that there are two different terminations due to the layered structure of Fe_3Si. The Fe termination is verified to be more stable than FeSi termination by performing the cohesive energies calculations. Thus, the Fe termination is considered in the present work. All the MgO barriers are fixed at 5 ML in the rest of the paper.

It is known that TMR ratio is a key parameter characterizing performance of MTJs. The *optimistic* TMR ratio is defined as $TMR = (G_P - G_{AP})/G_{AP}$, with G_P and G_{AP} being the total conductance for the magnetizations of two electrodes with parallel (PC) and anti-parallel configurations (APC), respectively. The calculated spin-polarized conductance and TMR ratios for a number of different MTJs are reported in Table I. All the relevant results for Fe/MgO/Fe(001) are also presented for comparison. We find that TMR ratio of Fe/MgO/Fe is around 3000%, which is in good agreement with that of Ref. 17. The giant TMR ratio in Fe/MgO/Fe originates from Δ_1 spin-filtering effect, as explained clearly in Refs. 3 and 4. Namely, incident Bloch wave functions from electrode will decay at symmetry-dependent rates through MgO barrier and the state with Δ_1 symmetry decays most slowly when compared with other states. Moreover, for *bcc* Fe, the Δ_1 band exists only in majority-spin channel at the Fermi level. Thus, a large conductance difference between PC and APC is obtained giving rise to the giant TMR ratio. The TMR ratio for the $Fe_3Si/MgO/Fe_3Si$ is very large, reaching ~5000%, which is larger than that of Fe/MgO/Fe. It is interesting and instructive to make a comparison between the $G_P^{\uparrow\uparrow}$ and $G_P^{\downarrow\downarrow}$. First of all, $G_P^{\uparrow\uparrow}$ is larger than $G_P^{\downarrow\downarrow}$ for Fe/MgO/Fe due to the contribution of the slowly decaying Δ_1 state. This is in sharp contrast to the case of $Fe_3Si/MgO/Fe_3Si$ for which $G_P^{\downarrow\downarrow}$ plays a dominant role in all spin channels. As Table I shows, $G_P^{\downarrow\downarrow}$ is about two orders of magnitude larger than that of other spin channels.

To understand the different conductance and TMR ratios presented above, we now examine transmission coefficients in the two-dimensional Brillouin zone (BZ), as plotted in Fig. 2. First, for Fe/MgO/Fe, the majority-spin in PC has a circular peak centered at $k_\parallel = (0, 0)$ due to the slow decay through Δ_1 state, whereas the minority-spin is characterized by sharp peaks-called *hot spots*, originating from resonant transmission through interface resonant states (IRSs).[18] In contrast, in the case of $Fe_3Si/MgO/Fe_3Si$, both the majority- and minority-spin in PC has negligible transmittance around the center of BZ, suggesting that there is no incoming Δ_1 Bloch states from Fe_3Si electrode. This can be confirmed from the symmetry-resolved band structures of bulk Fe_3Si, as plotted in Figs. 3(a) and 3(b). The bands have C_{4v} symmetry along the Δ direction (Γ-X). It is found only doubly degenerate Δ_5 (*pd*) band crosses the Fermi level E_F for majority-spin, while both Δ_5 and Δ_2 (*d*) bands cross E_F for minority-spin. On the other hand, the Δ_1 (*spd*) band for majority-spin locates at about 0.2 eV above E_F. There are two Δ_1 bands above E_F for minority-spin; one localizes around 0.9 eV and the other positions at 1.6 eV. Second, the resonance transmission peaks for minority-spin in PC can be distinctly suppressed by breaking the symmetry of MTJs,[19] e.g., by the interface oxidation or applied bias. To support this point, we constructed an asymmetric MTJ with one ML Fe 50% oxidized at one interface, namely $Fe_3Si/FeO/MgO/Fe_3Si$. As can be seen from Table I, the TMR reduces drastically from ~5000% to ~700% caused by the significant reduction of $G_P^{\downarrow\downarrow}$. Because in the case of symmetric MTJ, the localized interface states on the two Fe_3Si/MgO interfaces are at identical energies and when they align in energy, resonance transmission occurs. However, in the case of asymmetric MTJs, the two interface states are separated with an energy. Thus, resonance transmission is destroyed due to the mismatching of the two interface states. It can be further confirmed by the local density of states (LDOS) of an Fe atom at the interface shown in Fig. 4(a). For the symmetric MTJ, the minority-spin DOS shows a clear peak at around E_F, which can be attributed to the existence of interfacial states; on the contrary, there is no minority-spin DOS peak around E_F for the Fe atom in FeO

TABLE I. The calculated spin-polarized conductance G_σ (in units of e^2/h) and TMR ratios (in %) for a number of different MTJs. $G_P^{\uparrow\uparrow}$, $G_P^{\downarrow\downarrow}$ are the majority-spin and minority-spin conductance in PC, respectively. $G_{AP}^{\uparrow\downarrow}$, $G_{AP}^{\downarrow\uparrow}$ are the majority-to-minority and minority-to-majority conductance in APC, respectively. MgO barrier is chosen as 5 ML in all cases.

Structure	$G_P^{\uparrow\uparrow}$	$G_P^{\downarrow\downarrow}$	$G_{AP}^{\uparrow\downarrow}$	$G_{AP}^{\downarrow\uparrow}$	TMR (%)
Fe/MgO/Fe	1.23×10^{-3}	2.76×10^{-4}	2.32×10^{-5}	2.34×10^{-5}	3132
$Fe_3Si/MgO/Fe_3Si$	5.07×10^{-6}	1.84×10^{-4}	1.78×10^{-6}	1.78×10^{-6}	5211
$Fe_3Si/FeO/MgO/Fe_3Si$	1.05×10^{-5}	5.98×10^{-6}	8.78×10^{-7}	1.06×10^{-6}	750
T-$Fe_3Si/MgO/T$-Fe_3Si	1.08×10^{-3}	2.01×10^{-4}	2.71×10^{-5}	2.65×10^{-5}	2290

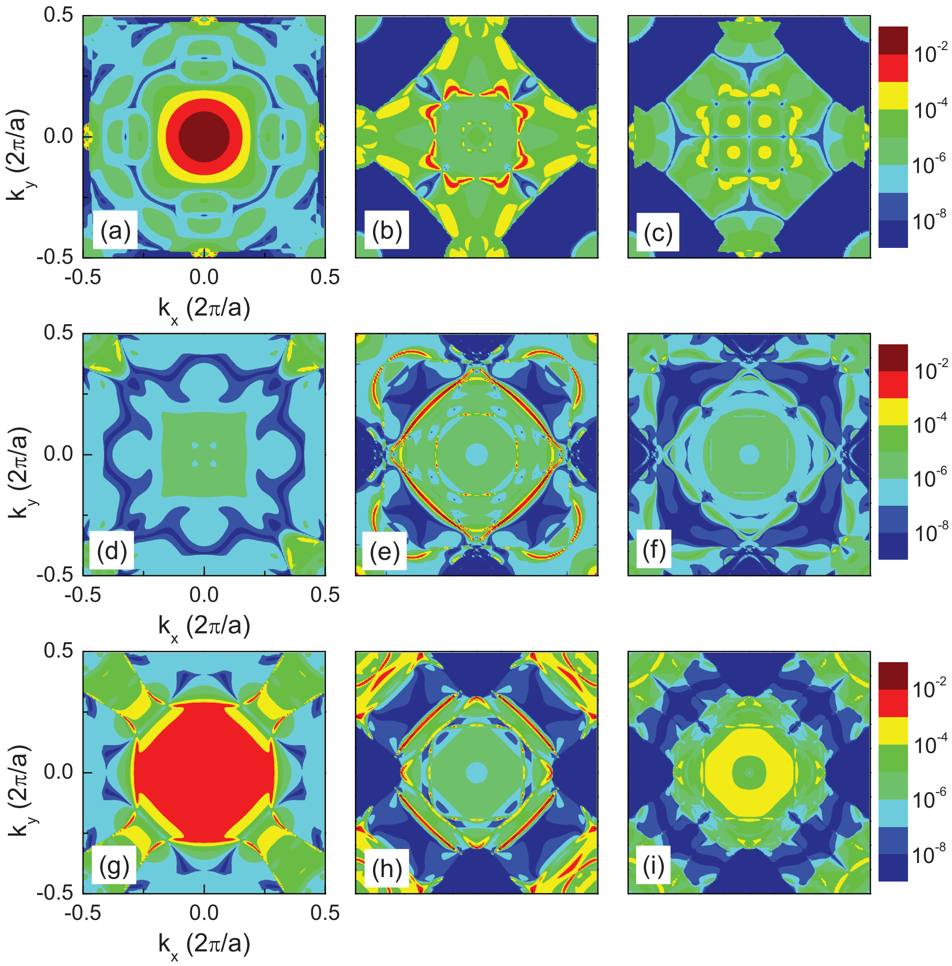

FIG. 2. Spin- and $k_{\|}$-resolved transmission coefficients for ((a)-(c)) Fe/MgO/Fe, ((d)-(f)) Fe_3Si/MgO/Fe_3Si and ((g)-(i)) *T*-Fe_3Si/MgO/*T*-Fe_3Si at the Fermi level. Panels from left to right are ((a), (d), (g)) for majority-to-majority and ((b), (e), (h)) for minority-to-minority in PC; ((c), (f), (i)) for majority-to-minority or minority-to-majority in APC.

layer. Fig. 4(b) plots the TMR ratio of Fe_3Si/MgO/Fe_3Si (blue circles) versus the bias. Note that in this condition the TMR ratio is defined as $TMR = (I_P - I_{AP})/I_{AP}$, with I_P (I_{AP}) being the total current for MTJ in PC (APC). We define the zero-bias TMR ratio using transmission coefficients. We see that the TMR ratio decreases very quickly with increasing the bias and drops to around 100% at a bias of 50 mV. This is because a small bias separates the two interface states[20] and, in consequence, suppresses the minority-spin resonance transmission in PC which is directly related to I_P. For MTJ-device application, output voltage V_{out} is another important parameter to characterize the magnitude of the output signal modulation.[21] V_{out} is defined as $V_{out} = V_b(G_P - G_{AP})/G_P$, where V_b is the applied bias. As plotted in the inset of Fig. 4(b) (blue circles), V_{out} increases roughly linearly with increasing V_b and then drops at around 40 mV due to the strong suppression of TMR ratio by bias.

To summarize, the giant TMR ratio of Fe_3Si/MgO/Fe_3Si decreases quickly with bias, which is detrimental to the output voltage V_{out}. This is the result of a strong suppression of resonant transmission through IRSs by bias. On the other hand, Δ_1 coherent transmission through MgO barrier is less affected by small bias in compared with IRSs.[17] Thus, it is favorable to V_{out} to achieve Δ_1 coherent transmission in Fe_3Si/MgO/Fe_3Si. We found that a slight in-plane compressive strain can drive the majority-spin Δ_1 band of Fe_3Si crossing E_F. We calculated the band structures of tetragonal Fe_3Si for a number of c/a ratios, where c and a are out-of-plane and in-plane lattice constants, respectively. Here, c/a

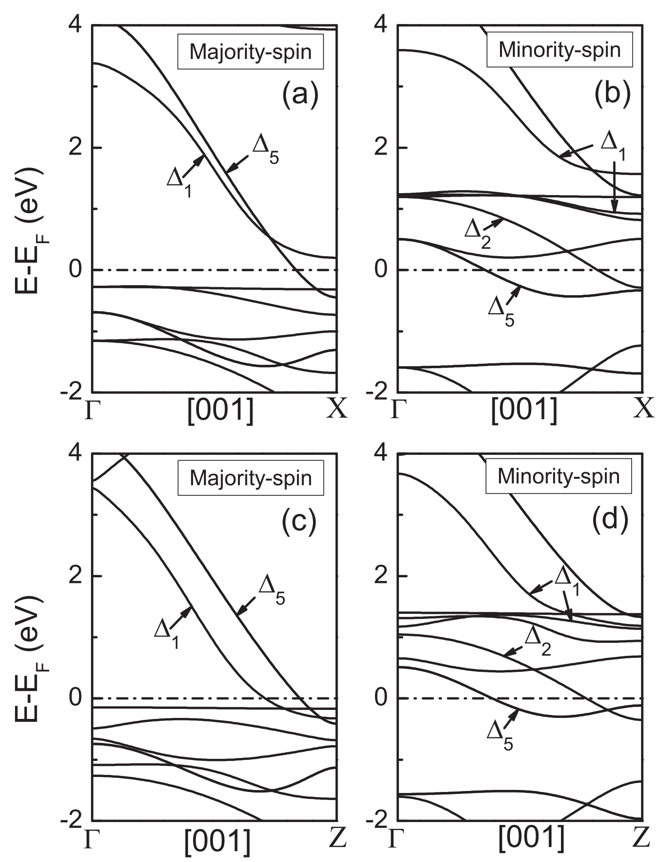

FIG. 3. Band structures of bulk ((a) and (b)) cubic Fe_3Si ($c/a = 1$) and ((c) and (d)) tetragonal Fe_3Si ($c/a = 1.07$). The Fermi level E_F has been aligned to zero.

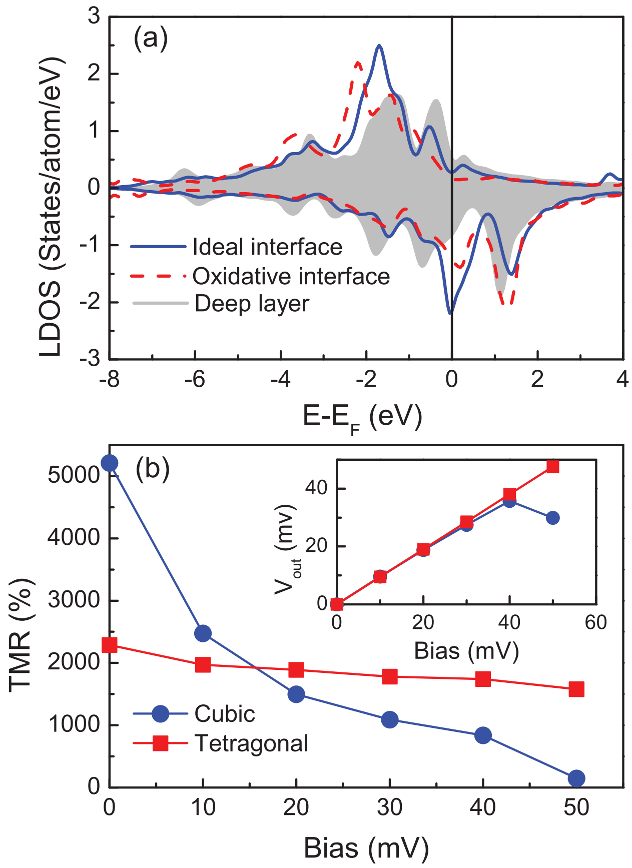

FIG. 4. (a) LDOS of an Fe atom at Fe_3Si/MgO, Fe_3Si/FeO/MgO interfaces; shaded plots are the LDOS of an Fe atom in the deep Fe layer, which is close to that of bulk. The majority- and minority-spin are plotted upward (positive) and downward (negative), respectively. (b) TMR ratios versus bias for Fe_3Si/MgO/Fe_3Si (blue circles) and T-Fe_3Si/MgO/T-Fe_3Si (red squares). Inset: Output voltage V_{out} versus bias.

ratio is determined by keeping the volume of the Fe_3Si unit cell fixed, namely $a^2c = a_0^3$ ($a_0 = 5.653$ Å). It is found that the majority-spin Δ_1 band crosses E_F, whereas minority-spin one does not when c/a ratio excess 1.04 (1.3% strain). Figs. 3(c) and 3(d) plot the band structure of tetragonal Fe_3Si with $c/a = 1.07$. In this case, a is chosen to be 3.905 Å, to model growth on the $SrTiO_3$(001) substrate, corresponding to 2.3% in-plane compressive strain. As expected, this new type of tetragonal Fe_3Si (T-Fe_3Si) reveals half-metal nature in terms of Δ_1 state, which is rather similar to that of *bcc* Fe. Then we calculated the transmission coefficients for T-Fe_3Si/MgO/T-Fe_3Si MTJ. As shown in Figs. 2(g)–2(i), the majority-spin in PC shows the expected broad peak around the center of BZ, whereas for the minority-spin and for APC there are negligible transmittance in the BZ, except for some resonance peaks at special $k_\parallel$ points. This is quite similar to that of Fe/MgO/Fe. As a consequence, giant TMR ratio of ~2000% is predicted originating from the Δ_1 spin-filtering effect, as reported in Table I. More importantly, as shown in Fig. 4(b) and its inset, the giant TMR ratio decays much slower with bias and, even at 50 mV bias, the TMR ratio is still over 1500%. This is due to the coherent transmission through the majority-spin Δ_1 channel, which is less affected by small bias when compared with IRSs. Thus, V_{out} increases linearly with increasing V_b and V_{out} is almost 1.6 times larger than that of Fe_3Si/MgO/Fe_3Si at 50 mV bias. This V_{out} difference will be expected to be further increased when the bias becomes larger.

In conclusion, we have calculated the TMR and spin-polarized transport in Fe_3Si/MgO/Fe_3Si(001) MTJs with two different Fe_3Si electrodes, i.e., cubic and tetragonal ones. Our results show that the giant TMR ratio for the former stems from the minority-spin interface resonant transmission, which can be dramatically reduced by breaking the symmetry of MTJs, e.g., by the interface oxidation or applied bias. For the latter, the tetragonal Fe_3Si reveals half-metal nature in terms of the Δ_1 state. Giant TMR ratio is predicted capitalizing on Δ_1 spin-filtering through MgO barrier and, more importantly, this giant TMR ratio drops much slower with bias in compared with former. Note that in real MTJs, the transport could be in either mixed ballistic and diffusive regime or diffuse regime due to the interface roughness and atom defects. Therefore, the TMR ratios might be smaller than the predicted values by taking into account of the diffuse scattering. Our studies provide some guidelines for achieving giant TMR ratio in Fe_3Si-based MTJ, which is a promising candidate as an MTJ element for designing STT-MRAM devices.

This work was supported by the State Key Project of Fundamental Research of Ministry of Science and Technology [MOST, No. 2010CB934400], National Natural Science Foundation [NSFC, Grant Nos. 11374351, 11174341, and 11222432], and Research Grant Council (Grant No. HKU 705212P) of HKSAR. The crystalline structure visualisation is plotted by using VESTA software.[22] We are grateful to the Shanghai Supercomputer Center for providing the computational facility.

[1]S. Ikeda, J. Hayakawa, Y. M. Lee, F. Matsukura, Y. Ohno, T. Hanyu, and H. Ohno, IEEE Trans. Electron Devices **54**, 991 (2007).
[2]S. Ikeda, J. Hayakawa, Y. Ashizawa, Y. M. Lee, K. Miura, H. Hasegawa, M. Tsunoda, F. Matsukura, and H. Ohno, Appl. Phys. Lett. **93**, 082508 (2008).
[3]W. H. Butler, X.-G. Zhang, T. C. Schulthess, and J. M. MacLaren, Phys. Rev. B **63**, 054416 (2001).
[4]J. Mathon and A. Umerski, Phys. Rev. B **63**, 220403(R) (2001).
[5]J. C. Slonczewski, J. Magn. Magn. Mater. **159**, L1 (1996).
[6]L. Berger, Phys. Rev. B **54**, 9353 (1996).
[7]S. Ikeda, K. Miura, H. Yamamoto, K. Mizunuma, H. D. Gan, M. Endo, S. Kanai, J. Hayakawa, F. Matsukura, and H. Ohno, Nature Mater. **9**, 721 (2010).
[8]Y. Huai, F. Albert, P. Nguyen, M. Pakala, and T. Valet, Appl. Phys. Lett. **84**, 3118 (2004).
[9]Z. Diao, D. Apalkov, M. Pakala, Y. Ding, A. Panchula, and Y. Huai, Appl. Phys. Lett. **87**, 232502 (2005).
[10]Y. Ando, K. Ichiba, S. Yamada, E. Shikoh, T. Shinjo, K. Hamaya, and M. Shiraishi, Phys. Rev. B **88**, 140406(R) (2013).
[11]A. Ionescu, C. A. F. Vaz, T. Trypiniotis, C. M. Gürtler, H. García-Miquel, J. A. C. Bland, M. E. Vickers, R. M. Dalgliesh, S. Langridge, Y. Bugoslavsky, Y. Miyoshi, L. F. Cohen, and K. R. A. Ziebeck, Phys. Rev. B **71**, 094401 (2005).
[12]Y. Fujita, S. Yamada, G. Takemoto, S. Oki, Y. Maeda, M. Miyao, and K. Hamaya, Jpn. J. Appl. Phys., Part 1 **52**, 04CM02 (2013).
[13]Y. N. Zhang, J. X. Cao, I. Barsukov, J. Lindner, B. Krumme, H. Wende, and R. Q. Wu, Phys. Rev. B **81**, 144418 (2010).
[14]J. Taylor, H. Guo, and J. Wang, Phys. Rev. B **63**, 245407 (2001).
[15]J. P. Perdew and A. Zunger, Phys. Rev. B **23**, 5048 (1981).
[16]G. Kresse and J. Furthmüller, Phys. Rev. B **54**, 11169 (1996). The cut-off energy of 500 eV, Perdew-Burke-Ernzerhof generalized gradient approximation (GGA) for the exchange correlation functional, and Monkhorst-Pack grid of 10 × 10 × 1 for k-point sampling were used. The atoms were

allowed to relax perpendicularly to the layers until the forces on each atom were smaller than 0.02 eV/Å.
[17]D. Waldron, V. Timoshevskii, Y. Hu, K. Xia, and H. Guo, Phys. Rev. Lett. **97**, 226802 (2006).
[18]O. Wunnicke, N. Papanikolaou, R. Zeller, P. H. Dederichs, V. Drchal, and J. Kudrnovský, Phys. Rev. B **65**, 064425 (2002).
[19]K. D. Belashchenko, J. Velev, and E. Y. Tsymbal, Phys. Rev. B **72**, 140404(R) (2005).
[20]I. Rungger, O. Mryasov, and S. Sanvito, Phys. Rev. B **79**, 094414 (2009).
[21]C. Tiusan, M. Sicot, M. Hehn, C. Belouard, S. Andrieu, F. Montaigne, and A. Schuhl, Appl. Phys. Lett. **88**, 062512 (2006).
[22]K. Momma and F. Izumi, J. Appl. Crystallogr. **44**, 1272 (2011).